

Green Synthesis of CdS/Ni_xS_y Nanoparticles as a Route Towards Sustainable and Scalable Photocatalysts

John Sakizadeh¹, Joseph P. Cline², Eva Wolfe¹, Ryan Thorpe³, Mark A. Snyder¹, Christopher J. Kiely^{1,2}, Steven McIntosh^{1*}

¹ Department of Chemical and Biomolecular Engineering, Lehigh University, Bethlehem, PA 18015, USA

² Department of Materials Science and Engineering, Lehigh University, Bethlehem, PA 18015, USA

³ Institute for Functional Materials and Devices, Lehigh University, Bethlehem, PA 18015, USA

*Corresponding author: mcintosh@lehigh.edu

Figure List

- Figure S1. UV-vis absorption spectra after adding lead acetate to solutions of 8 mM L-cysteine and 0.05 mg mL⁻¹ CSE in 100 mM Tris pH 9, Tris pH 7, and pH 5 acetate buffers allowing them to incubate at 37 °C for 2 h. The control for the experiment is L-cysteine and CSE in buffer after incubation but before the addition of 1 mM lead acetate. The increase in the absorbance above that of the control sample following lead acetate addition indicates that CSE is turning over some L-cysteine to produce HS⁻. 3
- Figure S2. UV-vis absorption spectra of 8 mM L-cysteine, 1 mM Ni(NO₃)₂, and 0.1 mg mL⁻¹ CSE in 100 mM pH 5 acetate buffer after incubating at 37 °C for 3 h within (i) a closed atmosphere reaction vessel and (ii) one being open to atmosphere. In the case of the closed atmosphere sample, the vial containing the biomineralization solution was tightly capped and the solution was filled to the top to eliminate any headspace in the container where H₂S can potentially escape. 3
- Figure S3. Time-on-line photocatalytic hydrogen evolution data for biomineralized CdS nanocrystals alone and biomineralized Ni_xS_y alone. 4
- Figure S4. XEDS mapping of the optimal CdS/Ni_xS_y catalyst containing 2.7 wt-% Ni_xS_y. .. a) High angle annular dark field image overlaid on the region with elemental maps of b) nickel, c) cadmium, d) oxygen, and e) sulfur. A highly dispersed Ni signal is present throughout the CdS particles. No individual Ni_xS_y particles or agglomerates were detected. 5
- Figure S5. Monitoring the time dependence of the absorbance at 800 nm after adding Ni_xS_y to the photocatalytic testing environment of 100 mM Na₂S, 100 mM Na₂SO₃, 50 mM Tris pH 9 buffer, and 4 mM L-cysteine (red). Adding Ni_xS_y to the reactor solvent reduces the absorbance at 800 nm over time, which indicates the dissolution of Ni_xS_y. 6

Figure S6. Adding biomineralized Ni_xS_y to the photocatalytic testing environment of 100 mM Na₂S, 100 mM Na₂SO₃, 50 mM Tris pH 9 buffer, and 4 mM L-cysteine (red) reduces absorbance at 800 nm relative to the case of adding biomineralized Ni_xS_y to water (blue) due to dissolution of Ni_xS_y. the dotted traces are the solvent without Ni_xS_y. 6

Figure S7. Extended time photocatalytic hydrogen evolution over a biomineralized CdS/Ni_xS_y catalyst with 2.7 wt-% of Ni_xS_y. A degradation in the photocatalytic hydrogen evolution rate is noticeable after about 2 h..... 7

Figure S8. Photocatalytic hydrogen evolution of CdS nanocrystals with 5 wt-% platinum and a 10 min or 30 min photodeposition time..... 8

Figure S9. a) Representative HAADF-STEM image of CdS with 5 wt-% platinum addition, b) high magnification image of platinum particle with a FFT inset fitting to [101] cubic platinum. c) XEDS point spectra showing the presence of S, Cd, and background Cu from the specimen grid, d) The same XEDS point spectra showing the presence of Pt and background Au from the specimen holder. 9

Table List

Table S1. Photocatalytic hydrogen evolution rates of CdS/Ni_xS_y with varying wt-% amounts of Ni_xS_y. 7

Table S2. Relevant preparative and catalytic data from previous literature reports of CdS/Ni_xS_y photocatalysts. 7

Table S3. Photocatalytic hydrogen evolution rates of CdS/Pt with varying amounts of platinum added. 8

Table S4. Photocatalytic hydrogen evolution data without normalization, normalized by the surface area, as well as represented by turnover frequency. For the surface area normalization, the surface area of the entire photocatalyst was used. The turnover frequency was calculated by dividing the nonnormalized hydrogen evolution rate by the moles of the added cocatalyst (Ni_xS_y or Pt)..... **Error! Bookmark not defined.**

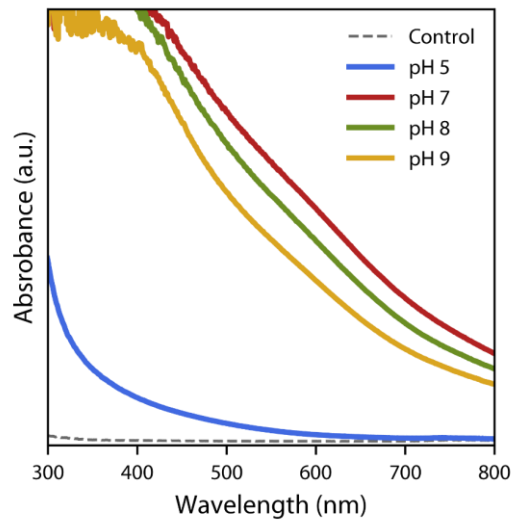


Figure S1. UV-vis absorption spectra after adding lead acetate to solutions of 8 mM L-cysteine and 0.05 mg mL⁻¹ CSE in 100 mM Tris pH 9, Tris pH 7, and pH 5 acetate buffers allowing them to incubate at 37 °C for 2 h. The control for the experiment is L-cysteine and CSE in buffer after incubation but before the addition of 1 mM lead acetate. The increase in the absorbance above that of the control sample following lead acetate addition indicates that CSE is turning over some L-cysteine to produce HS.

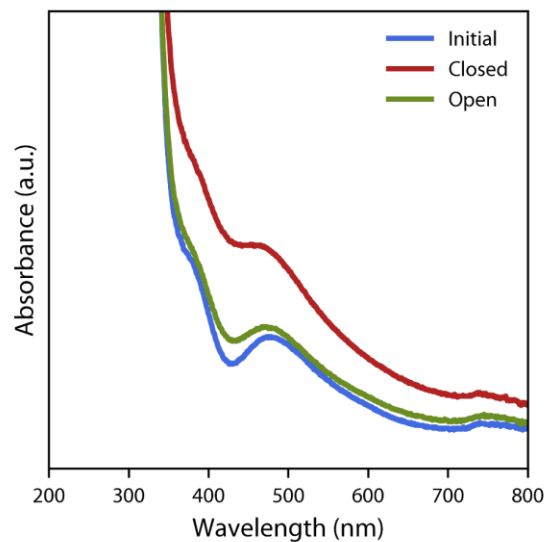


Figure S2. UV-vis absorption spectra of 8 mM L-cysteine, 1 mM Ni(NO₃)₂, and 0.1 mg mL⁻¹ CSE in 100 mM pH 5 acetate buffer after incubating at 37 °C for 3 h within (i) a closed atmosphere reaction vessel and (ii) one being open to atmosphere. In the case of the closed atmosphere sample, the vial containing the biomineralization solution was tightly capped and the solution was filled to the top to eliminate any headspace in the container where H₂S can potentially escape.

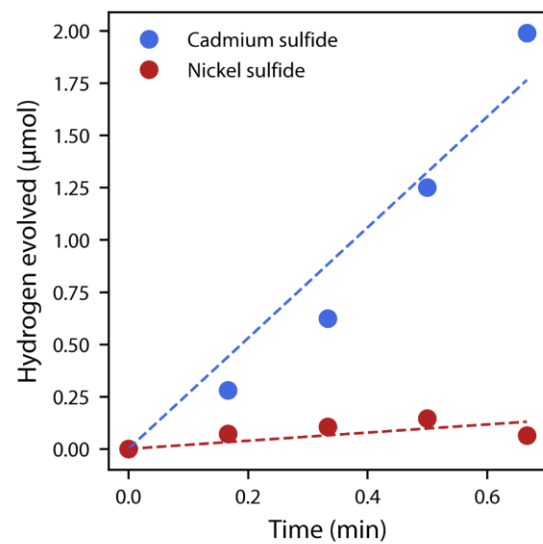


Figure S3. Time-on-line photocatalytic hydrogen evolution data for biomineralized CdS nanocrystals alone and biomineralized Ni_xS_y alone.

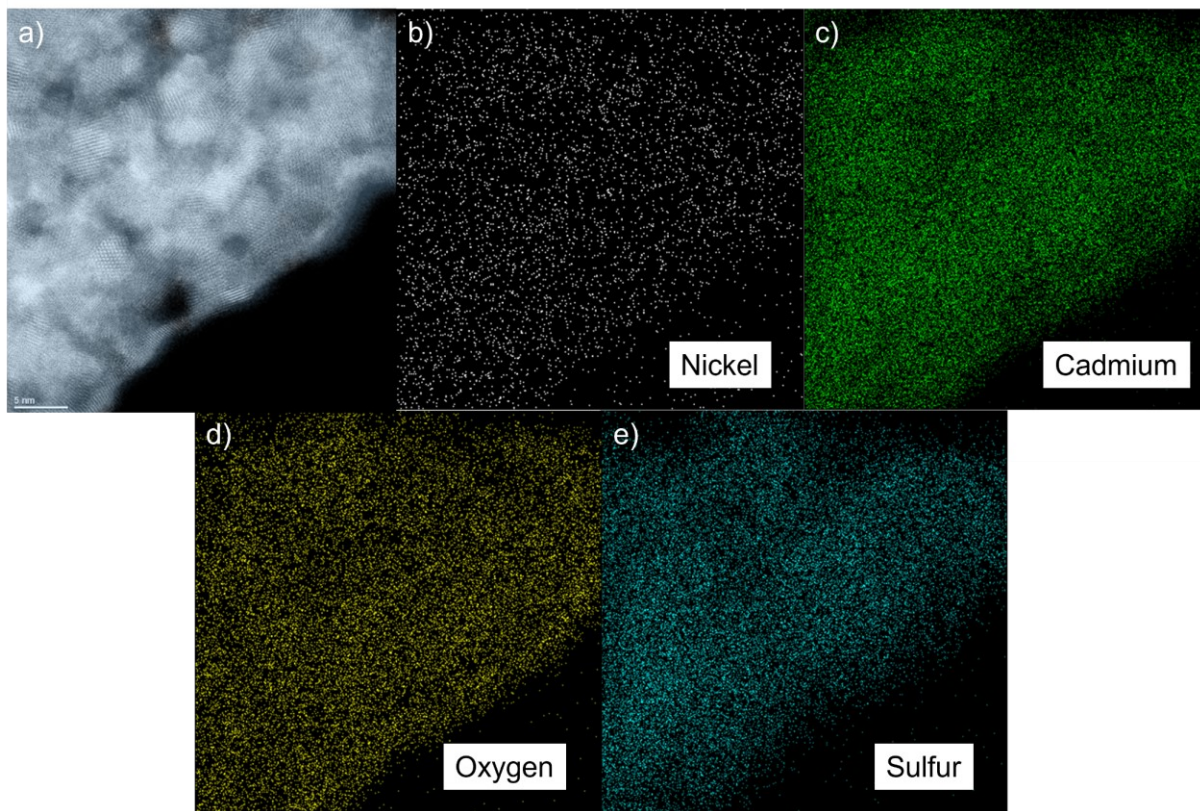


Figure S4. XEDS mapping of the optimal CdS/Ni_xS_y catalyst containing 2.7 wt-% Ni_xS_y. .. a) High angle annular dark field image overlaid on the region with elemental maps of b) nickel, c) cadmium, d) oxygen, and e) sulfur. A highly dispersed Ni signal is present throughout the CdS particles. No individual Ni_xS_y particles or agglomerates were detected.

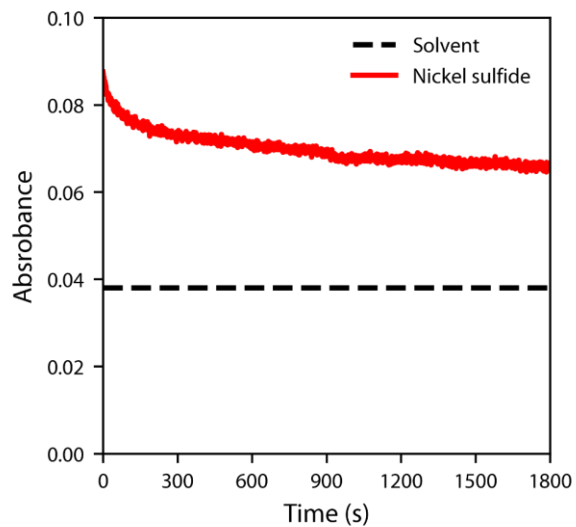


Figure S5. Monitoring the time dependence of the absorbance at 800 nm after adding Ni_xS_y to the photocatalytic testing environment of 100 mM Na_2S , 100 mM Na_2SO_3 , 50 mM Tris pH 9 buffer, and 4 mM L-cysteine (red). Adding Ni_xS_y to the reactor solvent reduces the absorbance at 800 nm over time, which indicates the dissolution of Ni_xS_y .

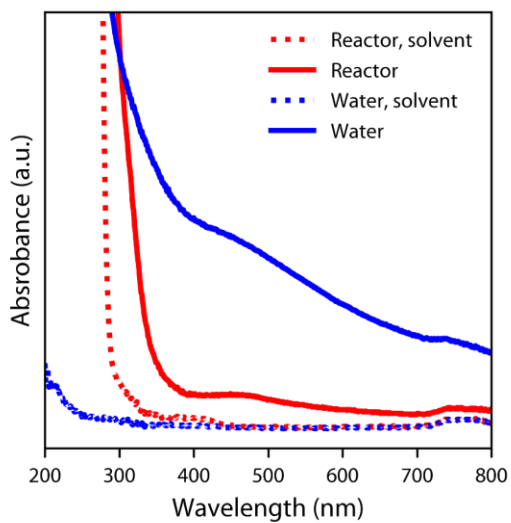


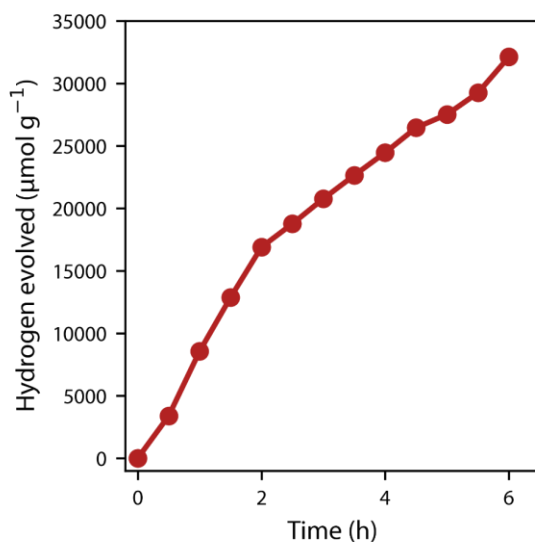
Figure S6. Adding biomineralized Ni_xS_y to the photocatalytic testing environment of 100 mM Na_2S , 100 mM Na_2SO_3 , 50 mM Tris pH 9 buffer, and 4 mM L-cysteine (red) reduces absorbance at 800 nm relative to the case of adding biomineralized Ni_xS_y to water (blue) due to dissolution of Ni_xS_y . the dotted traces are the solvent without Ni_xS_y .

Table S1. Photocatalytic hydrogen evolution rates of CdS/Ni_xS_y with varying wt-% amounts of Ni_xS_y.

Ni _x S _y (wt-%)	Photocatalytic hydrogen evolution rate (μmol h ⁻¹ g ⁻¹)
0.0%	1,400
0.2%	3,100
0.9%	7,800
1.8%	9,600
2.7%	10,500
3.5%	7,700

Table S2. Relevant preparative and catalytic data from previous literature reports of CdS/Ni_xS_y photocatalysts.

Reference	Material	Cadmium sulfide synthesis conditions	Nickel sulfide synthesis conditions	Photocatalytic hydrogen evolution rate (μmol h ⁻¹ g ⁻¹)
Liu et al. (2016) ¹	CdS/Ni _x S _y	Hydrothermal, 180 °C for 24 h	Reaction of Ni ²⁺ with Na ₂ S	25,000
Zhou et al. (2017) ²	CdS/NiS	Hydrothermal, 200 °C for 24 h	Hydrothermal, 200 °C for 24 h	25,000
Chen et al. (2020) ³	CdS/NiS	Solvothermal, 160 °C for 24 h	Hydrothermal, 120 °C for 12 h	400,000
Xu et al. (2017) ⁴	CdS/Ni _x S _y	Reaction of Cd ²⁺ with Na ₂ S	Reaction of Ni ²⁺ with Na ₂ S	25,000
Zhang et al. (2018) ⁵	CdS/NiS	Hydrothermal, 180 °C for 4 h	Hydrothermal, 180 °C for 4 h	30,000
Li et al. (2018) ⁶	CdS/NiS	Solvothermal, 180 °C for 24 h	Solvothermal, 180 °C for 12 h	1,500
Meng et al. (2018) ⁷	CdS/NiS	Solvothermal, 160 °C for 24 h	Hydrothermal, 160 °C for 24 h	6,000

**Figure S7.** Extended time photocatalytic hydrogen evolution over a biominedralized CdS/Ni_xS_y catalyst with 2.7 wt-% of Ni_xS_y.

A degradation in the photocatalytic hydrogen evolution rate is noticeable after about 2 h.

Table S3. Photocatalytic hydrogen evolution rates of CdS/Pt with varying amounts of platinum added.

Platinum wt-%	Photocatalytic hydrogen evolution rate ($\mu\text{mol h}^{-1} \text{g}^{-1}$)
0%	1,400
1%	2,200
5%	3,400
10%	3,000

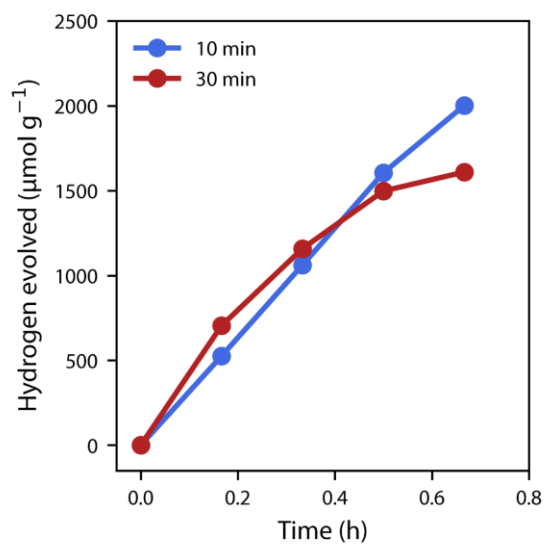


Figure S8. Photocatalytic hydrogen evolution of CdS nanocrystals with 5 wt-% platinum and a 10 min or 30 min photodeposition time.

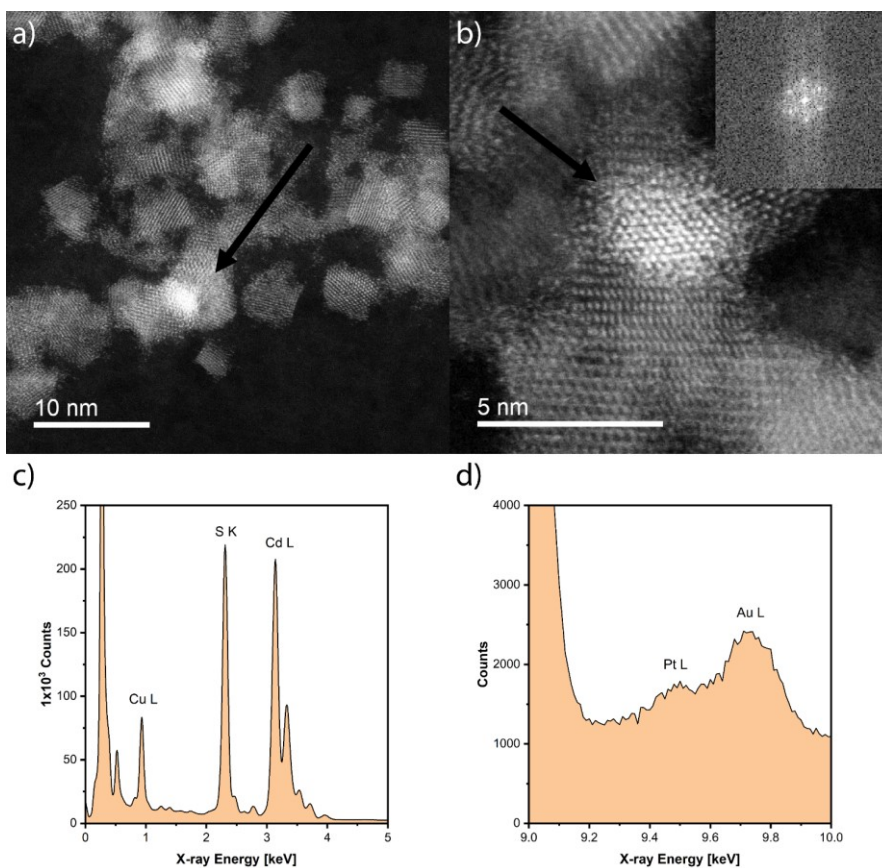


Figure S9. a) Representative HAADF-STEM image of CdS with 5 wt-% platinum addition, b) high magnification image of platinum particle with a FFT inset fitting to [101] cubic platinum. c) XEDS point spectra showing the presence of S, Cd, and background Cu from the specimen grid, d) The same XEDS point spectra showing the presence of Pt and background Au from the specimen holder.

Table S4. Photocatalytic hydrogen evolution data without normalization, normalized by the surface area, as well as represented by turnover frequency. For the surface area normalization, the surface area of the entire photocatalyst was used. The turnover frequency was calculated by dividing the non-normalized hydrogen evolution rate by the moles of the added cocatalyst (*i.e.*, Ni_xS_y or Pt).

Sample	Photocatalyst mass (mg)	Photocatalyst surface area ($\times 10^9 \text{ m}^2$)	H ₂ evolution rate ($\mu\text{mol h}^{-1}$)	Surface area normalized H ₂ evolution rate ($\mu\text{mol h}^{-1} \text{ m}^{-2}$)	TOF (s^{-1})
CdS	2.1 \pm 0.7	1.3 \pm 0.5	3.2 \pm 0.5	260 \pm 60	-
CdS + 5 wt-% Pt	2.2 \pm 0.2	1.3 \pm 0.1	6.9 \pm 0.6	523 \pm 9	0.0037 \pm 0.0003
CdS + 2.7 wt-% Ni _x S _y	2.2 \pm 0.2	1.4 \pm 0.2	26 \pm 4	1900 \pm 90	0.014 \pm 0.002

References

- 1 M. Liu, Y. Chen, J. Su, J. Shi, X. Wang and L. Guo, *Nat. Energy*, 2016, **1**, 1-8.
- 2 X. Zhou, H. Sun, H. Zhang and W. Tu, *Int. J. Hydrogen Energy*, 2017, **42**, 11199-11205.
- 3 Z. Chen, C. Cheng, F. Xing and C. Huang, *New J. Chem.*, 2020, **44**, 19083-19090.
- 4 Y. Xu, W. Tu, S. Yin, M. Kraft, Q. Zhang and R. Xu, *Dalton Transactions*, 2017, **46**, 10650-10656.
- 5 Y. Zhang, Z. Peng, S. Guan and X. Fu, *Appl. Catal. B-Environ.*, 2018, **224**, 1000-1008.
- 6 C. Li, H. Wang, S. B. Naghadeh, J. Z. Zhang and P. Fang, *Appl. Catal. B-Environ.*, 2018, **227**, 229-239.
- 7 S. Meng, Y. Cui, H. Wang, X. Zheng, X. Fu and S. Chen, *Dalton Transactions*, 2018, **47**, 12671-12683.